Acta Pharmacologica Sinica

www.nature.com/aps

ARTICLE

Discovery and biological evaluation of N-(3-(7-((2-methoxy-4-(4-methylpiperazin-1-yl)phenyl)amino)-4-methyl-2-oxo-2H-pyrimido[4,5-d][1,3]oxazin-1(4H)-yl)phenyl)acrylamide as potent Bruton's tyrosine kinase inhibitors

Meng-zhen Lai[1,2], Pei-ran Song[2,3,4], Dou Dou[5], Yan-yan Diao[5], Lin-jiang Tong[2,4], Tao Zhang[2,3,4], Hua Xie[2,4], Hong-lin Li[5] and Jian Ding[2,3,4]

Bruton's tyrosine kinase (BTK) is a key component of the B cell receptor (BCR) signaling pathway and plays a crucial role in B cell malignancies and autoimmune disorders; thus, it is an attractive target for the treatment of B cell related diseases. Here, we evaluated the BTK inhibitory activity of a series of pyrimido[4,5-d][1,3]oxazin-2-one derivatives. Combining this evaluation with structure-activity relationship (SAR) analysis, we found that compound **2** exhibited potent BTK kinase inhibitory activity, with an IC_{50} of 7 nM. This derivative markedly inhibited BTK activation in TMD8 B cell lymphoma cells and thus inhibited the in vitro growth of the cells. Further studies revealed that compound **2** dose dependently arrested TMD8 cells at G_1 phase, accompanied by decreased levels of Rb, phosphorylated Rb, and cyclin D1. Moreover, following treatment with compound **2**, TMD8 cells underwent apoptosis associated with PARP and caspase 3 cleavage. Interestingly, the results of the kinase activity assay on a small panel of 35 kinases showed that the kinase selectivity of compound **2** was superior to that of the first-generation inhibitor ibrutinib, suggesting that compound **2** could be a second-generation inhibitor of BTK. In conclusion, we identified a potent and highly selective BTK inhibitor worthy of further development.

Keywords: B cell receptor; Bruton's tyrosine kinase; ibrutinib; small-molecule inhibitor; B cell malignancies

Acta Pharmacologica Sinica (2020) 41:415–422; https://doi.org/10.1038/s41401-019-0250-8

INTRODUCTION

The Bruton's tyrosine kinase (BTK) protein is a nonreceptor tyrosine kinase belonging to the TEC family [1–3]. BTK is expressed in the cells of all hematopoietic lineages except for T and plasma cells [4, 5]. BTK is a critical downstream molecule of the B cell receptor (BCR) signaling pathway and plays an important role in the development of B cells [6, 7]. Dysregulation of BTK usually causes severe B cell related lymphomas and autoimmune diseases. These characteristics of BTK make it a very attractive treatment target for B cell malignancies [8–10].

There are two BTK inhibitors that have received marketing authorization for the treatment of B cell malignancies. The first-generation agent ibrutinib (PCI-32765) was approved by the US Food and Drug Administration (FDA) in 2013 to treat mantle cell lymphoma (MCL) and was subsequently approved for various indications, such as chronic lymphocytic leukemia (CLL), Waldenstrom's macroglobulinemia (WM), and marginal zone lymphoma [11–13]. However, ibrutinib not only irreversibly binds to BTK but also induces off-target inhibition [14–16], which might cause bleeding, rash, diarrhea, and atrial fibrillation during clinical treatment [17, 18]. To overcome the abovementioned limitations, the second-generation BTK inhibitor acalabrutinib (ACP-196), with better selectivity than ibrutinib, has been developed and received FDA approval in 2017 [19–22].

In our previous work, we identified a series of pyrimido[4,5-d][1,3]oxazin-2-one derivatives as potent mutant-selective epidermal growth factor receptor (EGFR) inhibitors [23] (Table 1). Recently, we unexpectedly found that compound **1** exhibited a moderate IC_{50} value of 28.8 nM against EGFR and an excellent IC_{50} value of 4.7 nM against BTK. To obtain selective BTK inhibitors, we began our study of pyrimido[4,5-d][1,3]oxazin-2-one–derived BTK inhibitors by investigating structure-activity relationships of previously synthesized pyrimido[4,5-d][1,3]oxazin-2-one irreversible EGFR inhibitors. Then, from the the kinase activity and selectivity results, we found that compound **2** could be a representative BTK inhibitor for further exploration.

[1]School of Pharmacy, Nanchang University, Nanchang 330006, China; [2]Division of Anti-tumor Pharmacology, State Key Laboratory of Drug Research, Shanghai Institute of Materia Medica, Chinese Academy of Sciences, Shanghai 201203, China; [3]School of Life Science and Technology, ShanghaiTech University, Shanghai 201210, China; [4]University of Chinese Academy of Sciences, Beijing 100049, China and [5]Shanghai Key Laboratory of New Drug Design, State Key Laboratory of Bioreactor Engineering, School of Pharmacy, East China University of Science and Technology, Shanghai 200237, China
Correspondence: Hua Xie (hxie@simm.ac.cn) or Hong-lin Li (hlli@ecust.edu.cn) or Jian Ding (jding@simm.ac.cn)
These authors contributed equally: Meng-zhen Lai, Pei-ran Song, Dou Dou.

Received: 7 March 2019 Accepted: 12 May 2019
Published online: 17 July 2019

Table 1. The chemical structure of compounds 1-8 and in vitro enzymatic inhibitory activities of 1-8, ibrutinib and ACP-196

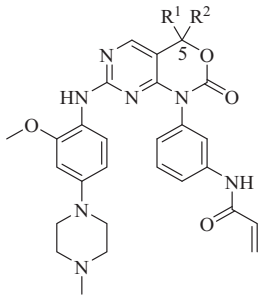

Compd.	R^1	R^2	Enzymatic inhibitory activity (IC_{50}, nM)	
			BTK	EGFR WT
1	H	H	4.7±0.3	28.8±9.3
2	H		7.0±4.1	47.4±12.7
3	H		14.0±5.4	23.4±9.7
4	H	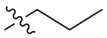	211.0±81.2	223.8±41.3
5	H		583.9±84.6	182.9±46.8
6			221.6±157.5	155.8±2.6
7			>10000	>1000
8	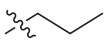	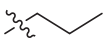	6417.0±1255.1	>1000
ibrutinib	/	/	0.6±0.1	1.2±0.3
ACP-196	/	/	8.6±2.3	>1000

[a]Data shown are collected from our previous study [23]

MATERIALS AND METHODS

Covalent docking

We used covalent docking to evaluate the binding pattern of the compound through the software of Maestro 10.1. We chose the PDB code 5P9L from the Protein Date Bank, and this PDB includes the crystal structure of BTK in complex with a small molecule CC-2922 [24]. As we expected, the compound binds to the ATP-bingding pocket of BTK, and the acrylamide of this compound proceeds Michael addition reaction with the thiol of Cys481. The position of inhibitor's core should be constrained to a maximum acceptable RMSD value of 1.0 Å from that of the binding ligand CC-292. The docking mode was defined as predicted pose, which find the precise docking pose through the full protocol. Glide was used to assess the affinity score between the inhibitor and BTK [25].

Cell culture and reagents

The human diffuse large B cell lymphoma (DLBCL) cell line TMD8 was obtained from the American Type Culture Collection (Manassas, VA, USA) and was cultured in RPMI-1640 medium (Gibco, USA) supplemented with 10% FBS (Gibco, USA). The TMD8 cell line was maintained at 37 °C in 5% CO_2.

Kinase assay
An enzyme-linked immunosorbent assay (ELISA) was used to evaluate the kinase inhibitory activity of compound **2**, ibrutinib, and ACP-196. The kinases were purchased from Eurofins (Brussels, Belgium). The experiment was performed according to standard ELISA procedures as previously described, and the absorbance was read at 490 nm with a multiwell spectrophotometer [26].

Cell proliferation assay
A Cell Counting Kit-8 (CCK8) assay was used to evaluate cell proliferation. TMD8 cells were seeded in 96-well plates at a density of 10,000 cells/well and incubated for 2 h, followed by exposure to compound **2**, ibrutinib, and ACP-196 at various concentrations for another 72 h. Subsequently, 10 μL of CCK8 solution (5 mg/mL) was added to each well for 1–2 h, and the results were assessed by measuring the absorbance at 450 nm using SoftMax Pro Software. The cell proliferation inhibition rate was calculated as follows: $[1-(A_{450\text{treated}}/A_{450\text{control}})]\times 100\%$ [27]. The logit method was used to obtain the IC_{50} values.

Western blot analysis
TMD8 cells were lysed in RIPA lysis buffer as previously described after washing with PBS [28]. Subsequently, TMD8 protein samples were used for Western blot analysis. Primary antibodies against the following proteins were used: actin (#3700), BTK (#8547), p-BTK (#87141), Rb (#9309), p-Rb (#2181), cyclin D1 (#2922), PARP (#9532S), caspase 3 (#9665S), and cleaved caspase 3 (#9664S). Antibodies were obtained from Cell Signaling Technologies (Cambridge, MA, USA).

Cell cycle analysis
TMD8 cells were seeded in 12-well plates, incubated for 2 h, and exposed to compound **2**, ibrutinib, and ACP-196 at various concentrations for another 48 h. A cell cycle analysis kit (Beyotime Biotechnology, Shanghai, China) was used to assess the cell cycle arrest of TMD8 cells. The cell cycle distribution was analyzed with a Becton-Dickinson FACSCalibur flow cytometer (BD Biosciences, San Jose, CA, USA), and the data were analyzed with Flow Jo software [29].

Cell apoptosis analysis
TMD8 cells were seeded in 12-well plates and incubated for 2 h and exposed to compound **2**, ibrutinib, and ACP-196 at various concentrations for another 72 h. An Annexin V-FITC kit (Vazyme Biotechnology, Nanjing, China) was used to detect the apoptosis of TMD8 cells. The cell apoptosis distribution was analyzed with a Becton-Dickinson FACS Calibur flow cytometer (BD Biosciences, San Jose, CA, USA), and the data were analyzed by Flow Jo software [29].

Statistical analysis
Data are presented as the means ± standard deviations (SDs). The significance of differences between experimental groups was evaluated with a two-tailed Student's *t* test. A *P* value of <0.05 was considered statistically significant. Significant differences are indicated as $^{*}P < 0.05$, $^{**}P < 0.01$, and $^{***}P < 0.001$.

RESULTS

SAR analysis
In our previous research, we identified a series of pyrimido[4,5-d][1,3]oxazin-2-one derivatives as epidermal growth factor receptor (EGFR) inhibitors [23], among which compound **1** also exhibited inhibitory activity against BTK. An in vitro enzymatic activity assay was performed, and the results are shown in Table 1. Compound **1** had a potent inhibitory effect on the enzymatic activity of BTK, with an IC_{50} value of 4.7 nM. The predicted covalent docking pose (Fig. 1a) generated via Maestro 10.1 by covalent docking shows that the pyrimido[4,5-d][1,3]oxazin-2-one core occupies the pocket adjacent to the hinge region, forming classic bidentate hydrogen bond interactions with the backbone of Met477. The lactone moiety of the central core participates in hydrogen bond networks with the surrounding residues, including a direct hydrogen bond interaction with Lys430 and indirect hydrogen bond interactions with Thr474 and Asp539, both of which are mediated by a water molecule. The left N-methylpiperazine ring extends to the solvent-exposed region, and it is poised in a suitable position to form favorable electrostatic interactions with Glu488 and hydrophobic interactions with Asn484. As expected, the electrophilic acrylamide group is covalently bonded to Cys481.

The hydrogen atom at the C-5 position of compound **1** directly points to the side chain of the gatekeeper residue Thr474, but there is still enough space to accommodate larger groups (Fig. 1a). Therefore, we discuss the effects of different substituents with varying volumes on the disparity in kinase activity between BTK and EGFR. On the one hand, diverse alkyl groups were introduced at the R^2 position, while R^1 was maintained as a hydrogen atom. Guided by this idea, compounds **2–5** were synthesized. On the other hand, R^1 and R^2 were simultaneously substituted with the same alkyl groups of different lengths, and the corresponding synthesized compounds were designated compounds **6–8**.

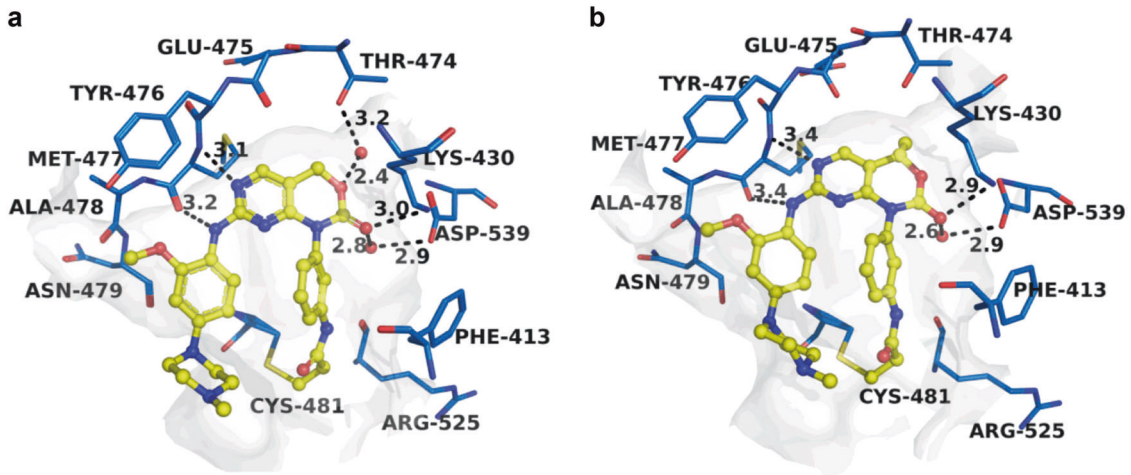

Fig. 1 Predicted docking poses of compounds **1** (**a**) and **2** (**b**) in the ATP binding pocket of BTK (PDB code 5P9L). Key residues around the binding pocket are displayed as marine lines, and the hydrogen bonds are presented as black dashed lines

The inhibitory potencies of compounds **1–8** against BTK kinase were evaluated using an ELISA-based kinase assay. When we changed only R^2, the kinase activity against BTK and the selectivity over EGFR showed a clear difference (Table 1). In general, the introduction of an alkyl group at the C-5 position led to a decrease in the activities of **1–8** against BTK. In addition, the kinase activity against BTK decreased as the length of the alkyl chain increased. However, compounds **1** and **2** still exhibited relatively high kinase activities against BTK, with IC_{50} values of 4.7 nM and 7.0 nM, respectively. Because our purpose was to discover highly selective BTK inhibitors, we considered not only the kinase activity against BTK but also the kinase activity against EGFR for the compounds reported in this study.

To further explore the effect of group size on BTK kinase activity and selectivity, the binding pose of compound **2** was also predicted with Maestro 10.1 (Fig. 1b). The methyl group of compound **2** lies directly beneath the side chain of the gatekeeper residue Thr474. Due to the limited space in the pocket near the gatekeeper residue, compound **3**, with an ethyl group at R^2, displayed a slight decrease in activity. Given the docking mode, we hypothesized that as the steric hindrance is enhanced, the kinase activity against BTK decreases. The results confirmed our hypothesis (Table 1). Compound **4**, with a propyl group at R^2, has an IC_{50} of 211.0 nM against BTK, indicating that this compound was 45-fold less potent than compound **1** and 30-fold less potent than compound **2**. The addition of the isopropyl group at R^2 in compound **5** resulted in an activity loss of ~124-fold relative to compound **1** (IC_{50} = 583.9 vs. 4.7 nM) and of 83-fold relative to compound **2** (IC_{50} = 583.9 vs. 7.0 nM).

In accordance with the activity trend observed above, compounds **6–8**, with two alkyl groups at the C-5 position, showed a greater loss of potency against BTK. In the ELISA-based kinase assay, the IC_{50} value of compound **6** indicated a 47-fold activity loss relative to compound **1**. Moreover, the addition of the second methyl group resulted in a 32-fold activity loss for compound **6** relative to compound **2** (IC_{50} = 221.6 vs. 7.0 nM). It should be noted that compounds **2–6**, to which a single alkyl group was introduced at the C-5 position, displayed higher activity against BTK than against EGFR. In contrast, compounds **6–8**, bearing two alkyl substituents at the same position, exhibited reversed selectivity between the two enzymes, providing significant clues for further optimization of selective BTK inhibitors.

As mentioned above, compound **2** potently inhibited the kinase activity of BTK, with an IC_{50} value of 7.0 nM, was weaker than ibrutinib, with an IC_{50} value of 0.6 nM but better than ACP-196, with an IC_{50} value of 8.6 nM. In addition, compound **2** exhibited greater than 6-fold higher selectivity for BTK than for EGFR (IC_{50} = 7.0 vs. 47.4 nM). Therefore, compound **2** was chosen for further evaluation at the cellular level.

Antiproliferative effects and target inhibition of compound 2 in TMD8 cells

We then investigated the antiproliferative activity of compound **2** in TMD8 lymphoma cells, which express high levels of BTK and are widely used to evaluate the antitumor effect of BTK inhibitors [18, 30–32]. Ibrutinib and ACP-196 were used as the positive control compounds [22, 33, 34]. The results revealed that compound **2** inhibited the proliferation of TMD8 cells with an IC_{50} value of 0.028 μM, indicating that compound **2** was slightly less potent than ibrutinib (IC_{50} = 0.010 μM) and ACP-196 (IC_{50} = 0.014 μM) (Table 2). Moreover, the Western blot analysis results revealed that compound **2**, ibrutinib and ACP-196 effectively suppressed the phosphorylation of BTK in TMD8 cells, confirming that the target inhibition by these compounds accounts for their antiproliferative activity (Fig. 2).

Table 2. In vitro antiproliferative effects of compound 2, ibrutinib and ACP-196 against TMD8 cells

Compd.	Cellular antiproliferative activity (IC_{50}, μM)
2	0.028 ± 0.014
Ibrutinib	0.010 ± 0.005
ACP-196	0.014 ± 0.004

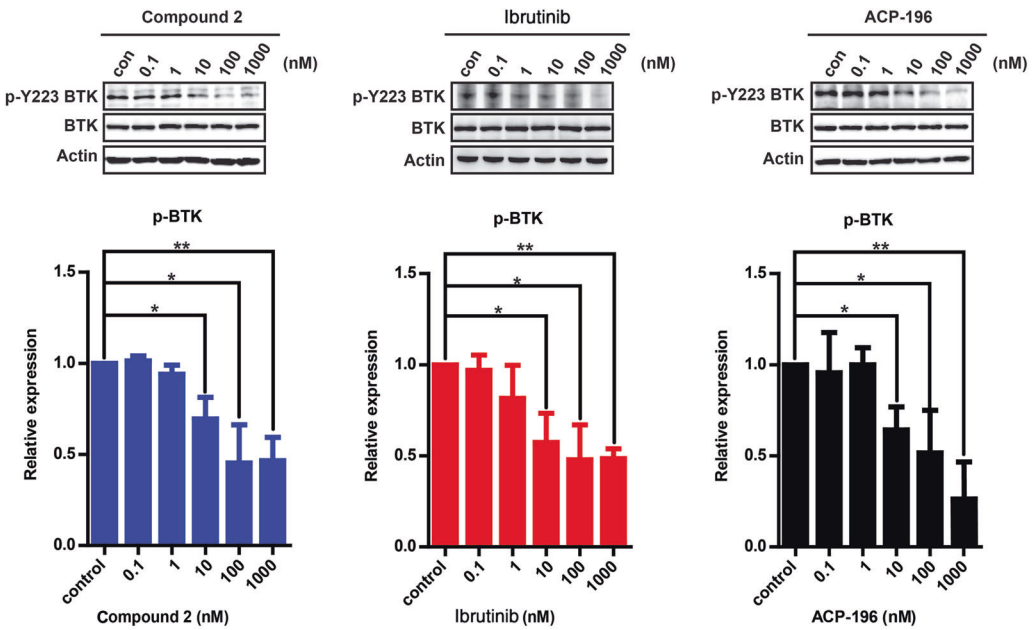

Fig. 2 The effects of compound **2**, ibrutinib, and ACP-196 on the phosphorylation of BTK at Tyr223 in TMD8 cells. Cells were treated with indicated concentrations of **2**, ibrutinib, and ACP-196 for 4 h and the total cell lysates were analyzed by Western blot analysis

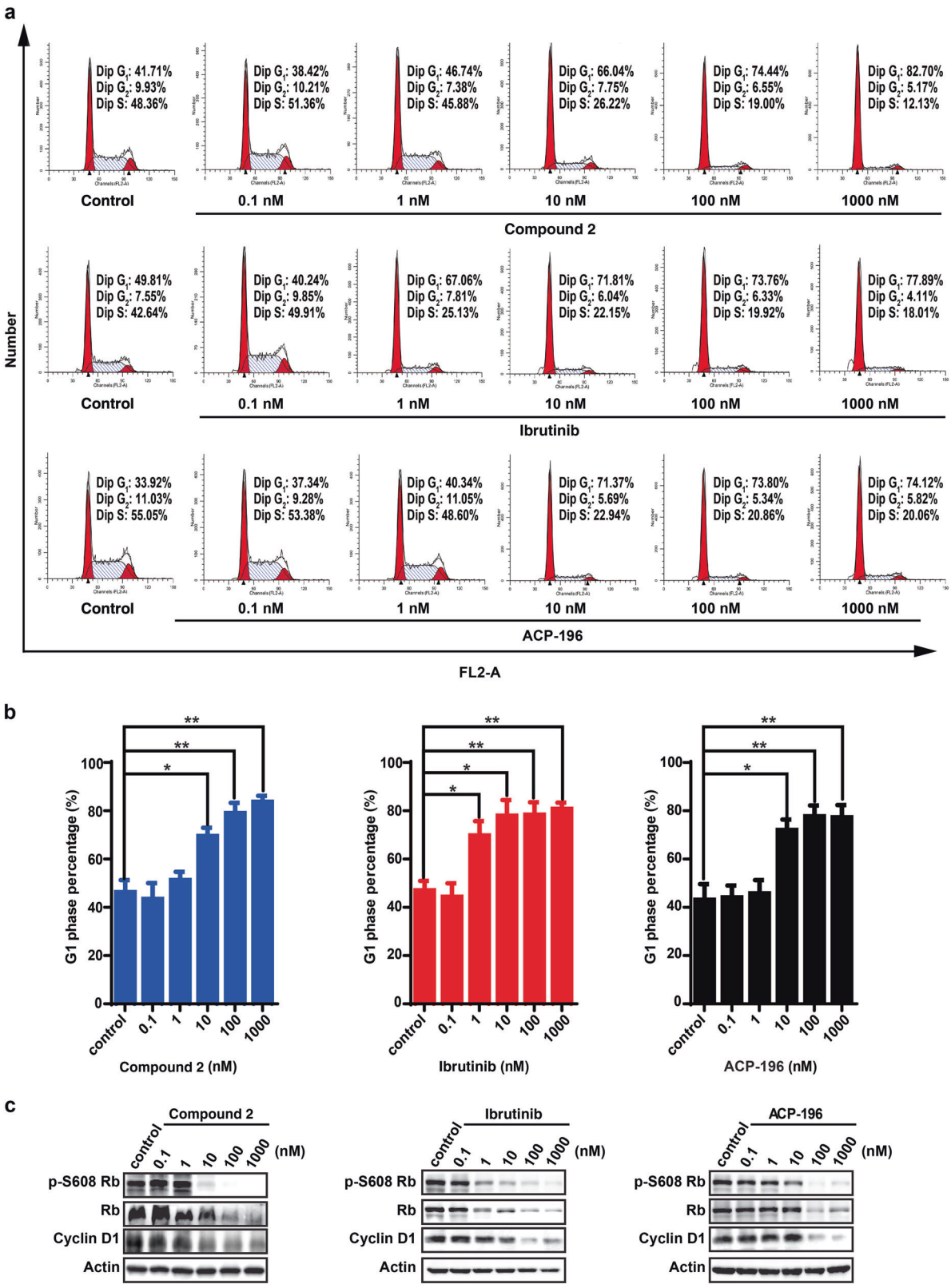

Fig. 3 Compound **2** blocked cell cycle progression at G_1 phase in TMD8 cells. **a** TMD8 cells were treated with indicated concentrations of **2**, ibrutinib and ACP-196 for 48 h. **b** The percentage of the G_1 phase cells was quantitatively depicted. Statistically significant differences were presented as $^*P < 0.05$, $^{**}P < 0.01$, compared with the control group. **c** TMD8 cells were treated with **2**, ibrutinib and ACP-196 for 48 h, and the total cell lysates were analyzed by Western blot to evaluate the alterations of G_1 phase related protein

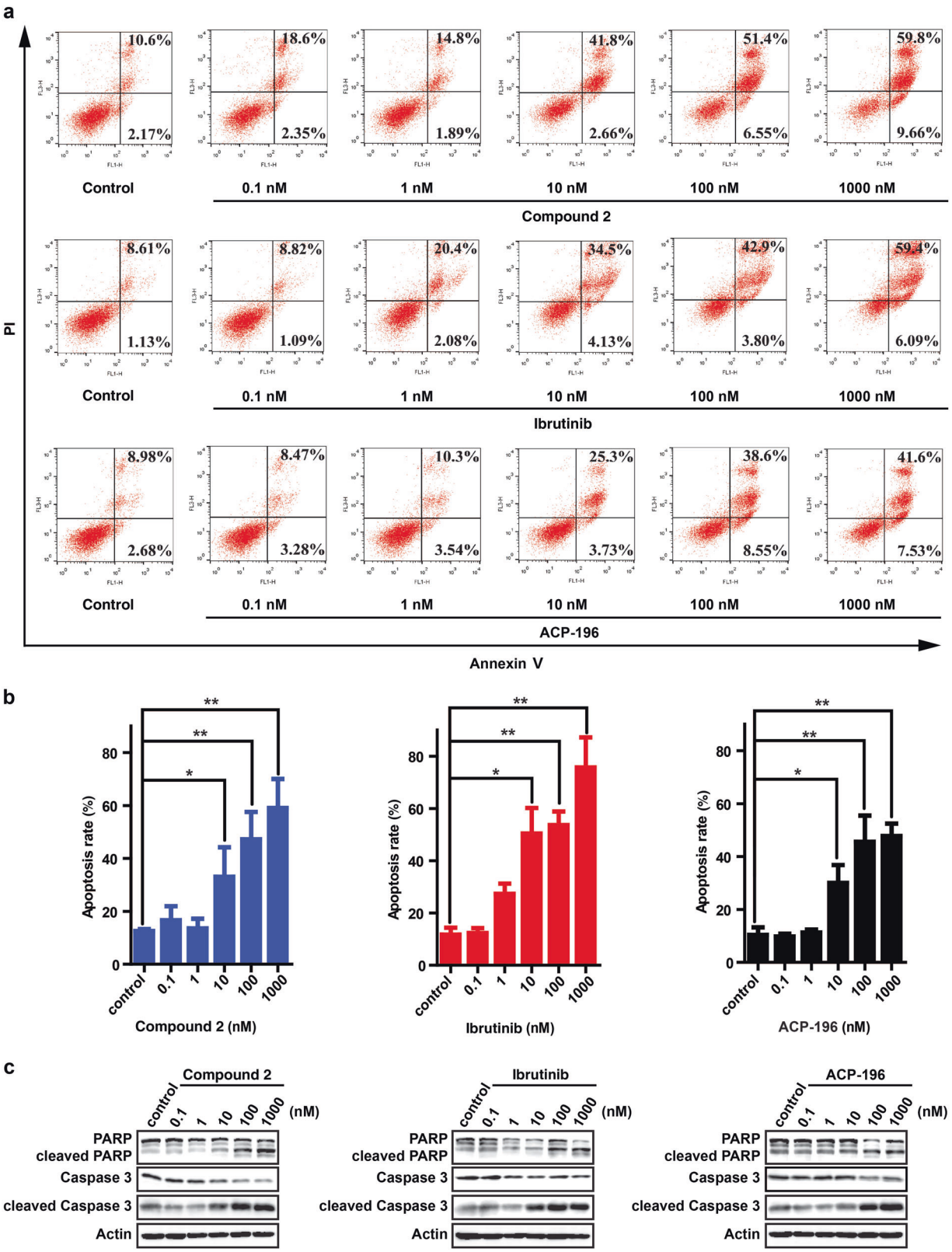

Fig. 4 Compound **2** induced cell apoptosis in TMD8 cells. **a** **2** significantly upregulated the apoptotic level of TMD8 cells equivalent to ibrutinib and ACP-196. **b** Apoptosis rates were quantitatively depicted. Statistically significant differences were presented as $^{*}P < 0.05$, $^{**}P < 0.01$, compared with the control group. **c** The expression of cleaved PARP and cleaved caspase 3 in TMD8 cells was determined by Western blot analysis

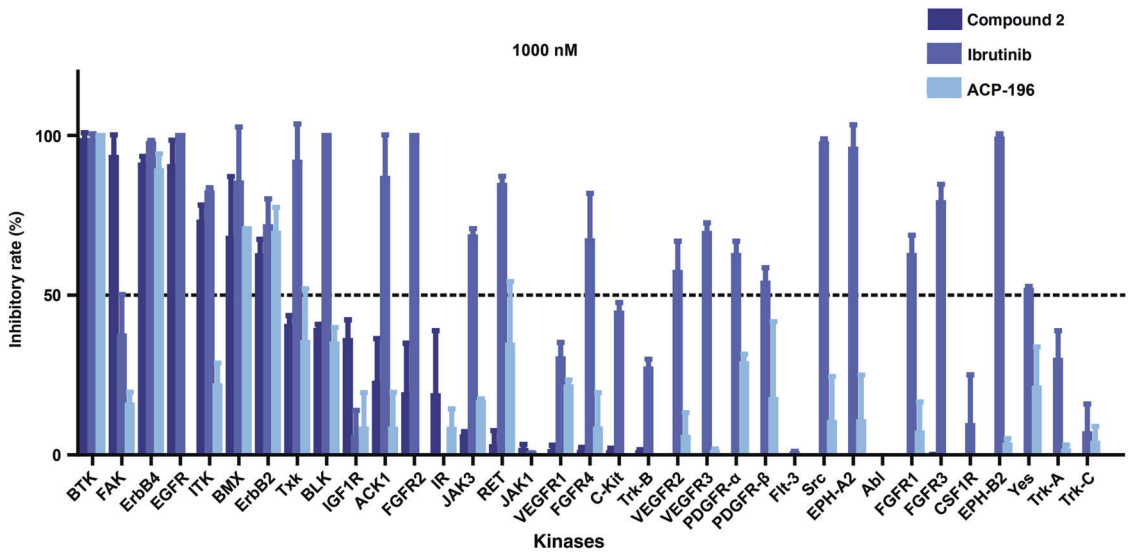

Fig. 5 Effects of compound **2**, ibrutinib, and ACP-196 against 35 kinases. Each compound was detected by ELISA assay at 1000 nM

Compound 2 arrested the cell cycle at the G_1 phase and induced apoptosis in TMD8 cells

To gain insight into the mechanism underlying the inhibition of cell growth by compound **2**, we further evaluated the effects of this compound on the cell cycle and apoptosis in TMD8 cells. After treatment with the indicated concentrations of the compounds for 48 h, compound **2** was found to markedly arrest cell cycle progression at the G_1 phase in a dose-dependent manner (Fig. 3a, b). Approximately 74.44% and 82.70% of the cells were arrested in G_1 phase when treated with concentrations of 100 nM and 1000 nM, respectively, equivalent to the results with ibrutinib and ACP-196. In agreement with these results, compound **2** caused a reduction in the levels of cell cycle-related proteins, including the Rb, phosphorylated Rb, and cyclin D1 proteins, consistent with the observation of G_1 arrest (Fig. 3c).

We then tested the effects of compound **2** on the apoptosis of TMD8 cells. Compound **2** triggered concentration-dependent apoptosis of the cells with apoptosis rates of 44.46%, 57.95%, and 69.46% for concentrations of 10 nM, 100 nM, and 1000 nM, respectively; the rate was 12.77% in untreated control cells (Fig. 4a, b). We further investigated the mechanism involved in the apoptosis induced by compound **2**, and the results showed that the cleavage of the poly (ADP-ribose) polymerase (PARP) and caspase 3 proteins was increased in a dose-dependent manner, indicating that compound **2** induced apoptosis through a caspase-related mechanism (Fig. 4c).

In conclusion, the results indicated that compound **2** exerted its antitumor effects through arresting the cell cycle at the G_1 phase and inducing apoptosis.

Kinase selectivity of compound 2

We then evaluated the kinase selectivity profile of compound **2** against a panel of 35 kinases available in our lab (Fig. 5). At a concentration of 1000 nM, compound **2** exhibited greater than 50% inhibition against seven kinases, including kinases sharing a conserved cysteine at the same position (such as EGFR, ErbB2, ErbB4, and ITK). Compound **2** did not appreciably inhibit the other kinases tested in this work. The kinase profile of compound **2** was quite similar to that of the 2nd generation BTK inhibitor ACP-196.

DISCUSSION

Lymphoma is a malignancy with high morbidity and mortality, and mature B cell lymphoma is the most common type of lymphoma [35]. The BCR is an important B cell antigen receptor that can regulate various B cell functions, including proliferation, survival, differentiation, and apoptosis [36]. The most important component in the BCR signaling pathway is BTK [37] and dysregulation of BTK generally causes severe B cell related lymphomas. Among the different treatment approaches, small molecule inhibitors targeting BTK might be an effective method to cure B cell lymphoma. To date, only two BTK inhibitors, ibrutinib, and ACP-196, have been approved for the treatment of BTK-induced diseases, and it is very important to develop novel BTK inhibitors with increased kinase selectivity and more potent antitumor activity.

In our study, the inhibitory efficacy of a series of pyrimido[4,5-d][1,3]oxazin-2-one derivatives against BTK was evaluated using an in vitro enzymatic activity assay. Compound **2** was identified as the most potent compound, with an IC_{50} of 7.0 nM against BTK. Moreover, this compound inhibited the activation of BTK in TMD8 lymphoma cells and thus repressed the in vitro growth of the cells. Further research showed that compound **2** induced cell death by triggering apoptosis and arresting the cell cycle at the G_1 phase. Interestingly, the kinase selectivity of compound **2** was superior to that of ibrutinib and equal to that of ACP-196 based on our data from a panel of 35 kinases. These data indicated that compound **2** might have fewer side effects than the first-generation BTK inhibitor ibrutinib. The activity of compound **2** against more kinases should be measured to exploit additional advantages of this compound. Moreover, it will also be meaningful to investigate the synergistic activity of compound **2** in combination with other drugs, such as antibody drugs and other BCR pathway inhibitors. Overall, our results identified compound **2** as a novel BTK inhibitor worthy of further investigation.

ACKNOWLEDGEMENTS

The research is supported in part by the National Key Research and Development Program (Grant 2016YFA0502304), the Special Program for Applied Research on Super Computation of the NSFC-Guangdong Joint Fund (the second phase) under grant No. U1501501, and the Fundamental Research Funds for the Central Universities.

AUTHOR CONTRIBUTIONS

MZL, PRS, DD, YYD, JD, and HIL designed the study; MZL, PRS, LJT, and TZ performed the research; DD and YYD contributed the compound; MZL, PRS, DD, and YYD analyzed the data; and MZL, PRS, DD, HIL, and HX wrote the paper.

ADDITIONAL INFORMATION

Competing interests: The authors declare no competing interests.

REFERENCES

1. Pal Singh S, Dammeijer F, Hendriks RW. Role of bruton's tyrosine kinase in B cells and malignancies. Mol Cancer. 2018;17:57.
2. Molina-Cerrillo J, Alonso-Gordoa T, Gajate P, Grande E. Bruton's tyrosine kinase (BTK) as a promising target in solid tumors. Cancer Treat Rev. 2017;58:41–50.
3. Rushworth SA, Pillinger G, Abdul-Aziz A, Rachel P, SM S, MM Y, et al. Activity of bruton's tyrosine-kinase inhibitor ibrutinib in patients with CD117-positive acute myeloid leukaemia: a mechanistic study using patient-derived blast cells. Lancet Haematol. 2015;2:204–11.
4. Smith CI, Baskin B, Humiregreiff P, Zhou JN, Olsson PG, Maniar HS, et al. Expression of bruton's agammaglobulinemia tyrosine kinase gene, BTK, is selectively down-regulated in T lymphocytes and plasma cells. J Immunol. 1994;152:557–65.
5. Seiler T, Dreyling M. Bruton's tyrosine kinase inhibitors in B-cell lymphoma: current experience and future perspectives. Expert Opin Invest Drugs. 2017;26:909–15.
6. Wu J, Zhang M, Liu D. Bruton tyrosine kinase inhibitor ONO/GS-4059: from bench to bedside. Oncotarget. 2016;8:7201.
7. Coutre SE, Furman RR, Flinn IW, Burger JA, Blum K, Sharman J, et al. Extended treatment with single-agent ibrutinib at the 420 mg dose leads to durable responses in chronic lymphocytic leukemia/small lymphocytic lymphoma. Clin Cancer Res. 2017;23:1149–55.
8. Valla K, Flowers CR, Koff JL. Targeting the B cell receptor pathway in non-hodgkin lymphoma. Expert Opin Invest Drugs. 2018;27:513–22.
9. Kondo K, Shaim H, Thompson PA, Burger JA, Keating M, Estrov Z, et al. Ibrutinib modulates the immunosuppressive CLL microenvironment through STAT3-mediated suppression of regulatory B cell function and inhibition of the PD-1/PD-L1 pathway. Leukemia. 2017;32:960–70.
10. Ge C, Wang F, Cui C, Su X, KKW To, Wang X, et al. PCI29732, a bruton's tyrosine kinase inhibitor, enhanced the efficacy of conventional chemotherapeutic agents in ABCG2-overexpressing cancer cells. Cell Physiol Biochem. 2018;48:2302–17.
11. Brown JR. Ibrutinib (PCI-32765), the first BTK (bruton's tyrosine kinase) inhibitor in clinical trials. Curr Hematol Malig Rep. 2013;8:1–6.
12. Rodgers TD, Reagan PM. Targeting the B-cell receptor pathway: a review of current and future therapies for non-hodgkin's lymphoma. Expert Opin Emerg Dr. 2018;23:111–22.
13. Paydas S. Management of adverse effects/toxicity of ibrutinib. Crit Rev Oncol Hematol. 2019;136:56–63.
14. Cheng S, Guo A, Lu P, Ma J, Coleman M, Wang YL, et al. Functional characterization of BTK(C481S) mutation that confers ibrutinib resistance: exploration of alternative kinase inhibitors. Leukemia. 2015;29:895–900.
15. Landau DA, Sun C, Rosebrock D, Herman SEM, Fein J, Sivina M, et al. The evolutionary landscape of chronic lymphocytic leukemia treated with ibrutinib targeted therapy. Nat Commun. 2017;8:2185.
16. Ruella M, Kenderian SS, Shestova O, Fraietta JA, Qayyum S, Zhang Q, et al. The addition of the BTK Inhibitor ibrutinib to anti-CD19 chimeric antigen receptor T cells (CART19) improves responses against mantle cell lymphoma. Clin Cancer Res. 2016;22:2684–96.
17. Patel V, Balakrishnan K, Bibikova E, Ayres M, Keating M, Wierda W, et al. Comparison of acalabrutinib, a selective bruton tyrosine kinase inhibitor, with ibrutinib in chronic lymphocytic leukemia cells. Clin Cancer Res. 2017;23:3734–43.
18. Wu J, Liu C, Tsui ST, Liu D. Second-generation inhibitors of bruton tyrosine kinase. J Hematol Oncol. 2016;9:80.
19. Awan FT, Jurczak W. Use of acalabrutinib in patients with mantle cell lymphoma. Expert Rev Hematol. 2018;11:495–502.
20. Jurczak W, Dlugosz-Danecka M, Wang M. Acalabrutinib for adults with mantle cell lymphoma. Expert Rev Clin Pharmacol. 2019;12:179–87.
21. Wu J, Zhang M, Liu D. Acalabrutinib (ACP-196): a selective second-generation BTK inhibitor. J Hematol Oncol. 2016;9:21.
22. Barf T, Covey T, Izumi R, Kar B, Gulrajani M, Lith B, et al. Acalabrutinib (ACP-196): a covalent bruton tyrosine kinase (BTK) inhibitor with a differentiated selectivity and in vivo potency profile. J Pharmacol Exp Ther. 2017;363:240–52.
23. Hao YJ, Jian KL, Qu R, Sun DH, Zhao ZJ, Chen Z, et al. Structure-guided design of c4-alkyl-1,4-dihydro-2hpyrimido[4,5-d][1,3]oxazin-2-ones as potent and mutant-selective epidermal growth factor receptor (EGFR) L858R/T790M inhibitor. Sci Rep. 2017;7:1–13.
24. Bender AT, Gardberg A, Pereira A, Johnson T, Wu Y, Grenningloh R, et al. Ability of bruton's tyrosine kinase inhibitors to sequester Y551 and prevent phosphorylation determines potency for inhibition of Fc receptor but not B-cell receptor signaling. Mol Pharmacol. 2017;91:208–19.
25. Richard A, Friesner JLB, Murphy Robert B, Halgren Thomas A, Klicic Jasna J, Mainz Daniel T, et al. Glide: a new approach for rapid, accurate docking and scoring. J Med Chem. 2004;47:1739–49.
26. Liu ZC, Wang ZL, Huang CY, Fu ZJ, Liu Y, Wei ZC, et al. Duhuo jisheng decoction inhibits SDF-1-induced inflammation and matrix degradation in human degenerative nucleus pulposus cells in vitro through the CXCR4/NF-κB pathway. Acta Pharmacol Sin. 2018;39:912–22.
27. Zheng YD, Bai G, Tang C, Ke CQ, Yao S, Tong LJ, et al. 7α,8α-epoxynagilactones and their glucosides from the twigs of podocarpus nagi: isolation, structures, and cytotoxic activities. Fitoterapia. 2018;125:174–83.
28. Zhang XX, Lin J, Liang TZ, Duan H, Tan XH, Xi BM, et al. The BET bromodomain inhibitor apabetalone induces apoptosis of latent HIV-1 reservoir cells following viral reactivation. Acta Pharmacol Sin. 2019;40:98–110.
29. Shi JJ, Chen SM, Guo CL, Li YX, Ding J, Meng LH, et al. The mTOR inhibitor AZD8055 overcomes tamoxifen resistance in breast cancer cells by down-regulating HSPB8. Acta Pharmacol Sin. 2018;39:1338–46.
30. Davis RE, Ngo VN, Lenz G, Tolar P, Young RM, P.B. R, et al. Chronic active B-cell-receptor signalling in diffuse large B-cell lymphoma. Nature. 2010;463:88–92.
31. Yahiaoui A, Meadows SA, Sorensen RA, Cui ZH, Keegan KS, Brockett R, et al. PI3Kδ inhibitor idelalisib in combination with BTK inhibitor ONO/GS-4059 in diffuse large B cell lymphoma with acquired resistance to PI3Kδ and BTK inhibitors. PLoS ONE 2017;12:221.
32. Kuo HP, Ezell SA, Hsieh S, Schweighofer KJ, Cheung LW, Wu S, et al. The role of PIM1 in the ibrutinib-resistant ABC subtype of diffuse large B-cell lymphoma. Am J Cancer Res. 2016;6:2489–501.
33. Dwivedi P, Muench DE, Wagner M, Azam M, Grimes HL, Greis KD, et al. Time resolved quantitative phospho-tyrosine analysis reveals bruton's tyrosine kinase mediated signaling downstream of the mutated granulocyte-colony stimulating factor receptors. Leukemia. 2019;33:75–87.
34. Zhang Z, Zhang DG, Liu Y, Yang DZ, Ran FS, Wang ML, et al. Targeting bruton's tyrosine kinase for the treatment of B cell associated malignancies and autoimmune diseases: preclinical and clinical developments of small molecule inhibitors. Arch Pharm. 2018;351:369.
35. Bray F, Ferlay J, Soerjomataram I, Siegel RL, Torre LA, Jemal A, et al. Global cancer statistics 2018: GLOBOCAN estimates of incidence and mortality worldwide for 36 cancers in 185 countries. Ca-Cancer J Clin. 2018;68:394–424.
36. Reiff SD, Muhowski EM, Guinn D, Lehman A, Fabian CA, Cheney C, et al. Noncovalent inhibition of C481S bruton's tyrosine kinase by GDC-0853: a new treatment strategy for ibrutinib resistant CLL. Blood. 2018;132:1039–49.
37. Tissino E, Benedetti D, Herman SEM, Hacken ET, Ahn IE, Chaffee KG, et al. Functional and clinical relevance of VLA-4 (CD49d/CD29) in ibrutinib-treated chronic lymphocytic leukemia. J Exp Med. 2018;215:681–97.